JOURNAL OF CATALYSIS 135, 99–114 (1992)

Mechanistic Kinetic Treatment of the Chain Growth Process in Higher Alcohol Synthesis over a Cs-Promoted Zn–Cr–O Catalyst

ENRICO TRONCONI, LUCA LIETTI, GIANPIERO GROPPI, PIO FORZATTI, AND ITALO PASQUON

Dipartimento di Chimica Industriale e Ingegneria Chimica "G. Natta" del Politecnico, Piazza L. Da Vinci 32, I-20133 Milano, Italy

Received April 12, 1990; revised September 26, 1991

A kinetic analysis has been performed of higher alcohol synthesis over Zn–Cr–O + 15% Cs_2O (w/w) using a reaction network strictly based on mechanistic evidence. This includes crossed aldol condensations of aldehydes and ketones and stepwise C_1 linear additions, both occurring in normal and "oxygen retention reversal" modes, as well as reversible ketonization reactions, and is consistent with chemical equilibrium constraints affecting the following reactions: methanol synthesis, water–gas shift, hydrogenation of carbonyl compounds, ester formation, and ketonization. Kinetic assumptions include reversible equilibrium adsorption of the reacting species on the catalyst sites, equilibrium of the C_1 intermediates with CO/H_2, and competition of water in adsorbing on the active sites. In line with available chemical data, different reactivities are attributed to the species participating in the chain growth process depending on their molecular structure (aldehydes versus ketones, linear versus branched). Using nine rate parameters, the model successfully describes the concentrations of 20 primary alcohols and ketones (and of the species related by chemical equilibria) as functions of contact time, temperature, pressure, and feed composition. The formation of about 50 additional compounds in trace amounts is also predicted, which are indeed not detected in the synthesis products. The parameter estimates show that aldol condensations are one order of magnitude faster than C_1 additions, indicate a greater reactivity of aldehydes than ketones, attribute a significant role to reverse ketonizations in the chain growth process in parallel to aldol condensations, and demonstrate the specific inhibiting action of water on condensations with oxygen retention reversal and ketonization. The apparent activation energies are very small for aldol condensations, ~63 kJ/mol for C_1 linear additions, and ~155 kJ/mol for ketonizations.

INTRODUCTION

The direct synthesis of mixtures of methanol and higher alcohols (designated higher alcohol synthesis, HAS) is effectively catalyzed by alkali-promoted methanol synthesis catalysts, operating either at low temperature (*1–5, 11*) or at high temperature (*6–11*).

The overall kinetics of HAS over a K-doped Zn–Cr oxide system have been treated on a lumped basis, the higher alcohols being regarded as a single pseudocomponent with average carbon number (*8*). A full description of the reacting system, however, requires a complementary approach aimed at modeling the kinetics of alcohol chain growth and the resulting distribution of C_{2+} oxygenates.

Kinetic treatments of the HAS product distributions have been proposed as extensions of the well-known Anderson–Schulz–Flory approach to the kinetics of the Fischer–Tropsch (FT) reaction. In this respect, the pioneering paper of Smith and Anderson (*12*), first presented a kinetic model describing C_{2+} alcohol product distributions, obtained over a commercial $Cu/ZnO/Al_2O_3$ methanol synthesis catalyst promoted with 0.5% K_2CO_3. It was proposed that the chain growth to higher alcohols occurs by one- or two-carbon addition at either the β or the α carbon atom of the growing alcohol intermediate, the species formed be-

0021-9517/92 $3.00

ing primary and secondary alcohols, respectively, i.e., the major classes of oxygenate products detected. Key kinetic assumptions included: (i) irreversible growth steps; (ii) termination of the chain growth process by irreversible desorption; (iii) first-order reaction rates with respect to the concentration of the growing intermediate, with rate constants independent of chain length; and (iv) steady-state conditions for all surface intermediates. It was found that the proposed scheme could describe quantitatively the observed alcohol distributions, and the values of the parameter estimates showed that α-addition was the slow step of the synthesis. However, the results were not discussed in terms of possible chemical mechanisms for the two main pathways of chain growth.

Smith *et al.* (*13*) have modified such a scheme to account for the synthesis of C_1–C_6 alcohols and methyl esters. Based on three mechanistic steps, including C_1 linear growth, β condensations of C_1–C_3 oxygenates and ester formation reactions, good agreement was claimed between model predictions and experimental distributions of C_{2+} oxygenates obtained over unpromoted and Cs-promoted Cu/ZnO. A modified, extended version of the Smith–Anderson kinetic treatment has also been applied to model the C_{2+} alcohol distribution obtained over an alkali-promoted Zn–Cr oxide high-temperature methanol synthesis catalyst (*14*). However, experimental evidence, at variance with two major assumptions of the Smith–Anderson approach, namely the irreversibility of all reaction steps and the pseudo-steady-state assumption for the concentrations of adsorbed intermediates, is now available.

Results of chemical enrichment experiments performed over both low-T (*12, 3*) and high-T (*7, 14*) modified methanol synthesis catalysts indicate that oxygenates added to the feed stream effectively participate in chain growth steps, which proves that the assumption of termination by irreversible desorption for the reaction products is invalid. This conclusion is also strongly supported by the fact that the methanol synthesis reaction as well as reactions involving ketones and primary alcohols ("ketonization" reactions) approach chemical equilibrium under HAS conditions (*15, 16*).

While the pseudo-steady-state assumption leads one to calculate an alcohol product distribution invariant with contact time, it is well known that the selectivities to various C_{2+} alcohols change significantly with contact time (*2*).

On the other hand, our understanding of the mechanistic features of the HAS over modified methanol synthesis catalysts has been greatly enhanced in recent years.

Klier and co-workers (*3, 5, 17, 18*) and Elliott and Pennella (*19, 20*) have independently investigated the mechanisms of C_2 and higher oxygenates synthesis over Cs-doped and undoped Cu/ZnO catalysts by isotopic labeling experiments: their results converge in showing that formation of the first C–C bond occurs through coupling of two C_1 oxygenate species related to methanol, while the successive faster chain growth to higher alcohols is dominated by aldol-type condensations, which are also responsible for the formation of ketones.

Regarding modified high-temperature methanol synthesis catalysts, consisting of mixed oxides of Cr, Zn, and/or Mn promoted with K or Cs, mechanistic features of the alcohol chain growth and of the related side reactions have been studied by temperature-programmed surface reaction (TPSR) techniques (*21–24*), IR spectroscopy (*25*), and chemical enrichment experiments (*7, 14*). The thermodynamic framework of the HAS has been systematically investigated a posteriori, and the classes of chemical reactions limited by chemical equilibrium have been identified (*15, 16*). The bulk of these data, together with specific information collected by continuous flow microreactor experiments using various oxygenate-containing feeds, has been eventually incorporated into a comprehensive reaction network for the HAS over high-T-modified methanol synthesis catalysts,

which accounts qualitatively for its extensive spectrum of products (*26*).

Based on such a reaction scheme, it is the purpose of the present paper to develop a kinetic treatment of the HAS over alkali-promoted high-T methanol synthesis catalysts, which overcomes the shortcomings of previous attempts, maintains a strict correspondence with the chemical aspects of the HAS as determined by independent measurements, and takes advantage of the considerable amount of mechanistic information that has been recently collected.

EXPERIMENTAL

The kinetic runs were performed in a Cu-lined fixed-bed tubular reactor, using a Cs-promoted Zn–Cr oxide catalyst. The experimental setup has been described in detail in previous papers (*8, 10, 16*).

The catalyst (Zn/Cr atomic ratio = 1/1) was prepared by coprecipitation from soluble salts, followed by filtering, washing, and drying at 110°C. The catalyst precursor was activated in N_2 at 400°C and then impregnated with 15% of Cs_2O (w/w) by the wet impregnation technique. Before the activity runs the catalyst was prereduced in the reactor in flowing H_2–N_2, with H_2 content and temperature progressively increased from 2 to 100%, and from room temperature to 400°C, respectively. XRD spectra of catalyst samples after the kinetic runs showed the existence of a microcrystalline spinel-like phase related to $ZnCr_2O_4$ and of better crystallized ZnO.

The analysis of the reaction products was specifically improved for the purposes of the present work, since the accurate quantitative estimation of oxygenates up to C_7–C_8 was recognized as essential to the kinetic analysis. Most of the various products were identified by GC–MS and GC–FTIR analyses on a sample of reactor effluent collected during a standard run (*21*). The identification of a few compounds was confirmed by adding known standards to the mixture of reaction products and analyzing it by high-resolution gas chromatography.

TABLE 1

Summary of Reaction Conditions for the Kinetic Runs

T (°C)	P (MPa)	GHSV (h^{-1})	H_2/CO feed	% CO_2 feed
365				
385	8.6	8,000	1/1	0
405				
385	8.6	8,000	1/1	0
		15,000		
		20,000		0
		25,000		3
405	8.6	8,000	1/1	0
405	8.6	8,000	1/2	0
			1/1	
			2/1	
			4/1	
405	8.6	8,000	1/1	0
	10.1			

The analysis of the condensed products was performed after each run using a GC equipped with capillary columns. Response factors were mainly estimated from the analysis of synthetic mixtures similar to typical mixtures of reaction products. When samples of a specific compound were not available, its response factor was determined by comparison with other similar species. The total number of detected products included typically over 100 compounds. A sample analysis of products of a typical run is presented in Ref. (*16*).

Experimental conditions for the kinetic runs are given in Table 1. The data allow identification of the effects of space velocity, CO_2 feed content, H_2/CO feed ratio, reaction temperature, and reaction pressure on the product distributions.

No catalyst deactivation was apparent from replicated runs in standard conditions at the end of the kinetic experiments.

DEVELOPMENT OF THE KINETIC MODEL

1. Reaction Network

The identification of the major chemical routes involved in the HAS over alkali-promoted high-T methanol synthesis catalysts has been the subject of a recent investigation in our laboratory, and will be reported in a companion paper (*26*). Here we

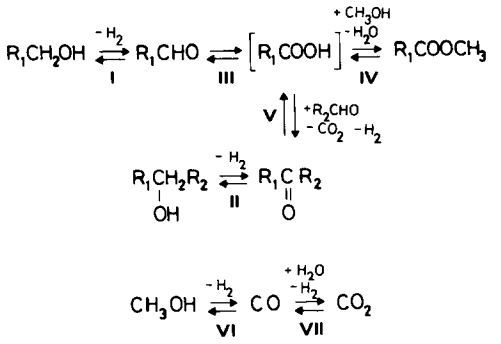

FIG. 1. Schematic representation of the equilibria prevailing under typical HAS conditions among the classes of oxygenated products.

briefly outline the main results to be included in the present treatment.

The thermodynamic analysis of the HAS product mixture (*16*) indicates that the gas-phase concentrations of the oxygenated species are related through various equilibrium constraints, as schematically shown in Fig. 1, including:

(a) hydrogenation equilibria between primary alcohols and aldehydes (I), secondary alcohols, and ketones (II);

(b) esterification equilibria between methyl esters, primary alcohols and methanol (I + III + IV);

(c) ketonization equilibria between ketones and aldehydes (III + V). In case of deviations from equilibrium, ketones typically exceed their equilibrium values, behaving as reactants in ketonization reactions and being decomposed into lower oxygenates, which further participate in the chain growth.

The methanol synthesis reaction (VI) and the water–gas shift reaction (VII) are also essentially at equilibrium under typical HAS conditions.

Superimposed on this thermodynamic constrained background is a kinetic controlled chain growth mechanism, which is dominated by the two following chemical routes (see Fig. 2):

(a) aldol-type condensations of carbonyl compounds, occurring according both to the "normal" mode (β_N) and to the "oxygen retention reversal" mode (β_{ORR}) (*5, 17*); in the ORR mode, the aldol intermediate of the condensation undergoes hydrogenation/dehydration of the carbonyl group and retention of the anionic oxygen rather than dehydration with loss of the hydroxyl oxygen;

(b) stepwise C_1-additions on the carbonyl carbon atom, which are also assumed to occur both in the normal (α_N) and in the reversal (α_{ORR}) mode (*18*); in particular, this route, with R_1CCHO replaced by HCHO in Fig. 2, is responsible for the first C–C bond formation of the chain growth process ($C_1 \rightarrow C_2$ step).

In the resulting chain growth scheme illustrated in Fig. 2 the contribution to the distribution of higher oxygenates associated with reversible ketonizations (Γ) has also been included. According to this scheme, ketones are generated by aldol condensations and by C_1 additions, both occurring with the oxygen retention reversal mechanism, while they are partially decomposed by reverse ketonizations. Notably, in Fig. 2 and in the following treatment the species participating in the chain growth are indicated conventionally as primary alcohols and ketones. Actually, primary alcohols and

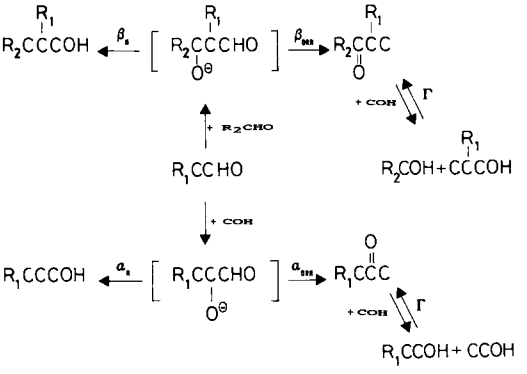

FIG. 2. Schematic representation of the chain growth mechanism in HAS. For clarity, hydrogen atoms have been omitted in the molecular formulas.

aldehydes, as well as secondary alcohols and ketones, are kinetically indistinguishable because of the hydrogenation equilibria mentioned above. The choice of primary alcohols and ketones results from their greater abundance in the products as compared to aldehydes and secondary alcohols, respectively.

An important role in determining the product distribution is played by the water–gas shift (WGS) reaction, which is responsible for the low water content of the HAS product mixture. In fact, while the stoichiometry of each growth step involves formation of H_2O molecules, these are in good part converted with formation of CO_2. Large CO_2 feed contents are known to adversely affect the overall carbon selectivity to C_{2+} alcohols (*8*), and also exhibit specific effects on the distribution of oxygenated products (*16*).

The formation of hydrocarbons and ethers has been neglected since only minor traces of such compounds were detected.

The mechanism in Fig. 2 provides the basis for the kinetic treatment of HAS illustrated in the following sections.

2. *Kinetic Assumptions*

2.1. Equilibrium adsorption on the catalyst surface is invoked for all species participating in the chain growth,

$$\Theta_i = K_{ad} C_i \Theta^*, \qquad (1)$$

where C_i and Θ_i are the concentrations of species i in the gas phase and at the catalyst surface, respectively, while K_{ad} represents an adsorption equilibrium constant equal for all species, and Θ^* is the surface concentration of free sites. The assumption of adsorption equilibrium is consistent with the reversible desorption of several HAS products demonstrated by chemical enrichment experiments where intermediate products were added to the reactor feed, as well as with the various chemical equilibria prevailing under HAS conditions.

2.2. Based on the thermodynamic analysis of the HAS, it is further assumed that methanol, CO_2, and H_2O are at equilibrium with CO + H_2 throughout the catalyst bed. As a consequence of assumptions 2.1 and 2.2, then, all C_1 species, either adsorbed or in the gas phase, are essentially at equilibrium with each other. For the purposes of the kinetic description, this makes unnecessary any assumptions on the specific nature (e.g., formate, formyl, formaldehyde, methoxide, methanol) of C_1 intermediates involved in the chain growth steps.

2.3. Aldol condensations and C_1 linear additions are regarded as irreversible steps with first-order kinetics in the surface concentration of one reactant and in the gas-phase concentration of the other (Eley–Rideal mechanism),

$$r_{ij} = k_{ij} \Theta_i C_j, \qquad (2)$$

which is compatible with the chemical nature of the reaction mechanisms. The resulting rate expression,

$$r_{ij} = \frac{k_{ij} K_{ad} C_i C_j}{1 + \Sigma_m K_{ad} C_m + K_W C_{H_2O}}, \qquad (3)$$

where competition of water for adsorption on the active sites of the catalyst has also been included by introducing a specific adsorption equilibrium constant K_W, can account for the observed inhibiting effect of the reaction products on the rates. The local H_2O concentration was estimated from the equilibrium of the WGS reaction.

Preliminary regression results showed that saturation effects were negligible for aldol condensations and C_1 linear additions occurring in the normal mode, but were significant for reactions with oxygen retention reversal. Also, it was found that in the ORR case the adsorption of water dominates the denominator in Eq. (3). Accordingly, the following rate expressions were assumed in the kinetic analysis of aldol condensations and C_1 additions:

$$\text{Normal mode:} \quad r_{ij} = k_{ij} K_{ad} C_i C_j \qquad (4)$$

$$\text{ORR mode:} \quad r_{ij} = \frac{k_{ij} K_{ad} C_i C_j}{1 + K_W C_{H_2O}} \qquad (5)$$

2.4. The rate expression for ketonization reactions, which are limited by equilibrium (*16*), is based on similar kinetic assumptions, but accounts also for the reverse reaction

$$r_{ij,\text{ket}} = k_\Gamma \Theta_{\text{ket}} C_1 p_{H_2} - k_{-\Gamma} \Theta_i C_j$$

$$= k_\Gamma K_{\text{ad}} C_1 p_{H_2} \frac{C_{\text{ket}} - \dfrac{C_i C_j}{p_{H_2} C_1 K_{\text{ket},ij}}}{1 + K_W C_{H_2O}}. \quad (6)$$

In Eq. (6), $K_{\text{ket},ij}$ is the equilibrium constant for the ketonization reaction with stoichiometry involving a ketone + methanol to give the two lower alcohols i and j, e.g.,

$$H_2 + CH_3OH + CH_3(CO)CH_2CH_3 \rightleftharpoons C_2H_5OH + C_3H_7OH. \quad (7)$$

Based on independent observations that ketonizations and ORR reactions are similarly inhibited by CO_2-rich syngas and similarly promoted by alkali-metal addition to the catalyst, the same parameter K_w used in the kinetic expression for ORR condensations, Eq. (5), has been used in Eq. (6) for ketonization reactions.

3. Reactivities of the Species Participating in Chain Growth

The rate constants k_{ij} in Eqs. (4), (5) have been differentiated on the basis both of the type of the reaction and of the nature of the reacting molecules, as illustrated below. The resulting set of kinetic parameters is defined in Table 2.

3.1. Aldol condensations. Such reactions involve a nucleophilic and an electrophilic reactant and may occur according to either the normal or the ORR mode.

Based primarily on TPSR and flow microreactor data, in the present kinetic treatment it is assumed that both C_{2+} aldehydes and ketones can act as nucleophilic species, whereas C_1–C_4 aldehydes have been considered as possible electrophilic reactants (*26*).

Aldehydes and ketones have been assigned different reactivities as nucleophilic agents by introducing a factor Ω, defined as the ratio of the rate constant for ketones to the rate constant for aldehydes ($k_{\beta,N}$) in aldol condensation reactions. On the basis of literature indications for homogeneous reactions and of data obtained in microreactor experiments over a Zn–Cr–O + K catalyst (*26*), it is expected that $\Omega < 1$. Based on TPSR results and on the outcome of chemical enrichment experiments with *i*-butanol added to the CO + H_2 feed, condensations involving α-branched nucleophilic agents (e.g., *i*-butanal, 2-methylbutanal) have been excluded.

Due to possible steric effects, the reactivity of nucleophilic species with β-branching with respect to the carbonyl group (e.g., 3-methylbutanal) has also been differentiated by introducing a specific rate constant, $k_{\beta,B}$.

Concerning the electrophilic reactants, the same reactivity has been assumed for all the linear aldehydes, independent of the carbon number, while for 2-methylpropanal the influence of the methyl substituent in the α-position on the electrophilic character of the molecule with respect to the reactivity of straight chain aldehydes is described by means of a factor Φ:

$$\frac{k_{\beta,i-C4}}{k_{\beta,N}} = \Phi. \quad (8)$$

The ratio of the rate constant for ORR aldol condensations ($k_{\beta,ORR}$) to the rate constant for "normal" condensations ($k_{\beta,N}$) has been regarded as a fixed parameter, Ω_{ORR}, independent of the reacting species. A single exception is made when the nucleophilic reagent is a compound with a methyl group in α-position with respect to the carbonyl group (e.g., ethanol, acetone). In this case, a specific enhancing effect for the ORR reactions is manifest over alkali-promoted catalysts, as revealed by literature data (*5*). This is accounted for by using a specific rate constant, $k_{\beta,E}$. Finally, ORR aldol condensations involving *i*-butanal as the electrophilic species have been ruled out since no clear evidence was available for their occurrence (*26*).

TABLE 2

Kinetic Parameters Used in the Description of the Oxygenate Product Distribution

Nucleophilic reactant	Electrophilic reactant		Rate constant	
Aldol condensations (β):			N mode	ORR mode
R_1CH_2CHO	HCHO—nC_3CHO		$k_{\beta,N}$	$\Omega_{ORR}\ k_{\beta,N}$
	C—C—CHO C		$\Phi\ k_{\beta,N}$	
CH_3CHO	HCHO—nC_3CHO		$k_{\beta,N}$	$k_{\beta,E}$
	C—C—CHO C		$\Phi\ k_{\beta,N}$	$\Phi\ k_{\beta,E}$
R_1CHCH_2CHO R_2	HCHO—nC_3CHO		$k_{\beta,B}$	$\Omega_{ORR}\ k_{\beta,B}$
	C—C—CHO C		$\Phi\ k_{\beta,B}$	—
CH_3COCH_2R	HCHO—nC_3CHO	(on —CH_2—)	$\Omega\ k_{\beta,N}$	$\Omega\ \Omega_{ORR}\ k_{\beta,N}$
		(on CH_3—)	$\Omega\ k_{\beta,N}$	$\Omega\ k_{\beta,E}$
	C—C—CHO C	(on —CH_2—)	$\Omega\ \Phi\ k_{\beta,N}$	—
		(on CH_3—)	$\Omega\ \Phi\ k_{\beta,N}$	$\Omega\ \Phi\ k_{\beta,E}$
C_1 linear growth (α):			N mode	ORR mode
HCHO	R_1CHO		k_α	$\Omega_{ORR}\ k_\alpha$
	R_1—C—CHO C		$\Phi\ k_\alpha$	$\Phi\ \Omega_{ORR}\ k_\alpha$
Ketonization (Γ):				
R_1CH_2CHO	R_2CHO		k_Γ	

3.2. C_1 linear growth. These reactions involve a common C_1 nucleophilic species and different electrophilic intermediates (*18*). While all the aldehydes were assumed to participate in this class of reactions, C_1 linear additions on ketones were ruled out on the basis of chemical enrichment experiments. The same reactivity, represented by the rate constant k_α, has been attributed to all the electrophilic intermediates, but for species branched at the α-position with respect to the carbonyl group (e.g., *i*-butanal), for which a specific rate constant ($k_{\alpha,B}$) has been introduced in consideration of possible electronic or steric effects. It has been further assumed that

$$k_{\alpha,B}/k_\alpha = k_{\beta,i-C_4}/k_{B,N} = \Phi. \qquad (9)$$

This implies that the presence of a substituent in the α-position of an aldehydic reagent affects similarly its electrophilic character in aldol condensations and in C_1 linear additions.

Also, the same parameter Ω_{ORR} defined for aldol condensations has been applied to represent the ratio of the rate of C_1 addition in ORR mode to the rate in normal mode ($k_{\alpha,ORR} = \Omega_{ORR}\ k_\alpha$). A significant exception is provided by the $C_1 \rightarrow C_2$ step, for which we have assumed that only the ORR mechanism prevails. In fact, the normal mechanism would require in this case an unfavorable H-abstraction from the carbonylic carbon:

$$HCHO + {}^-HC{=}O \rightarrow$$
$$[{}^-OCH_2CHO] \xrightarrow{-OH^-} [CH_2{=}C{=}O].$$

For higher intermediates, hydrogen atoms in β-position become available, whose abstraction results in the formation of a C=C bond conjugate with the carbonyl group:

$$CH_3CHO + {}^-HC{=}O \rightarrow$$
$$[{}^-O(CH_3)CHCHO] \xrightarrow{-OH^-}$$
$$[CH_2{=}CHCHO] \xrightarrow{+H_2} CH_3CH_2CHO.$$

3.3. Ketonization reactions. It has been assumed that all of the aldehydes participate in ketonizations. However, condensation of two α-branched aldehydes (e.g., *i*-butanal) have been excluded, based on TPSR evidence (*23, 24*). Also, we assume that the molecular structure of the species participating in these reactions does not affect the rate of reaction, so that only one rate parameter (k_Γ) needs to be introduced.

In summary, a total of nine independent rate parameters ($k_{\beta,N}$, $k_{\beta,B}$, $k_{\beta,E}$, Ω_{orr}, Ω, k_α, Φ, k_Γ, K_W) are required for the proposed kinetic description of the HAS system.

4. Reactor Model and Distribution Equations

For the calculation of the model responses, a simple isothermal pseudohomogeneous plug flow reactor model,

$$\frac{dC_i}{d(1/\mathrm{GHSV})} = \sum_{m=1}^{N_{Ri}} v_{im} r_{im}, \qquad i = 1, N_C \tag{10}$$

was adopted, where C_i is the concentration of species i, GHSV is the space velocity, N_{Ri} is the number of reaction steps involving species i, and v_{im} is the stoichiometric coefficient of species i in mth reaction. Isothermal operation was assumed based on the essentially flat measured axial T-profiles. Molar contraction of the reacting mixture was neglected, the overall CO conversion being always below 15%.

Fourteen C_{2+} primary alcohols and six ketones were identified in the C_2–C_7 range as the major products obtained in the HAS over the Cs-promoted Zn–Cr–O catalyst and were selected as the experimental responses of the kinetic analysis. Such compounds are listed in Table 3 along with their concentrations in the products of a typical kinetic run.

Determination of the 20 model responses, however, requires calculation of the related concentrations for a number of other compounds participating in the chain growth network. Thus, for a model solution integration of a set of $N_C = 42$ material balance equations had to be performed.

TABLE 3

Experimental Responses Used in Kinetic Modeling of the HAS Over Cs-Promoted Zn–Cr–O Catalyst

Reaction conditions: T = 385°C, P = 8.6 MPa, GHSV = 8000 h^{-1}, % CO_2 feed = 0.

i	Species	$C_i/C_{methanol}$
1	Ethanol	1.33×10^{-2}
2	1-Propanol	4.69×10^{-2}
3	1-Butanol	3.28×10^{-3}
4	1-Pentanol	1.64×10^{-3}
5	1-Hexanol	5.30×10^{-4}
6	2-Me-1-propanol	1.05×10^{-1}
7	2-Me-1-butanol	6.04×10^{-3}
8	2-Me-1-pentanol	5.13×10^{-3}
9	2-Me-1-hexanol	1.52×10^{-3}
10	3-Me-1-butanol	9.50×10^{-4}
11	3-Me-1-pentanol	2.30×10^{-4}
12	4-Me-1-pentanol	6.80×10^{-4}
13	2,3-diMe-1-butanol	7.80×10^{-4}
14	2,4-diMe-1-pentanol	3.17×10^{-3}
15	2-Butanone	9.80×10^{-4}
16	3-Pentanone	1.66×10^{-3}
17	3-hexanone	2.30×10^{-4}
18	3-Me-2-butanone	4.60×10^{-4}
19	2-Me-3-pentanone	1.88×10^{-3}
20	2,4-diMe-3-pentanone	3.30×10^{-4}

The mass balance equations (10) were rearranged dividing through by C_1 to eliminate the concentration of the C_1 species, replacing C_i with $y_i = C_i/C_1$; i.e., the outlet concentrations of the oxygenates ratioed to the methanol concentration. Correspondingly, the rate parameters were redefined as

$$\begin{aligned} \beta_N &= k_{\beta,N} K_{ad} C_1 \\ \beta_B &= k_{\beta,B} K_{ad} C_1 \\ \beta_E &= k_{\beta,E} K_{ad} C_1 \\ \alpha &= k_\alpha K_{ad} C_1 \\ \Gamma &= k_\Gamma K_{ad} C_1 p_{H_2} \\ A_W &= K_W C_1 . \end{aligned} \tag{11}$$

Considering also the ratios of rate constants

Ω, Ω_{ORR}, Φ, a total of nine kinetic parameters is used. In the above expressions, C_1 is taken to be constant along the reactor axis because of the equilibrium assumption for methanol.

In the mass balances for primary alcohols, terms associated with the generation of the corresponding aldehydes were neglected, since the concentration of such species was generally lower by one order of magnitude for thermodynamic reasons (*16*). In the case of mass balances for ketones, however, the contributions due to the formation of the corresponding secondary alcohols were not negligible and were accounted for by incrementing the net rate of ketone formation by (1 + SK). Here, SK represents the average expected molar ratio (secondary alcohol/ketone) based on hydrogenation equilibria. This factor was estimated a priori from thermodynamic data as a function of temperature and hydrogen partial pressure, a typical value being SK = 0.4 at T = 405°C, P = 8.6 MPa, H_2/CO = 1/1 (*16*). Likewise, the equilibrium constants for ketonization reactions $K_{ket,ij}$ appearing in Eq. (6) were estimated from thermodynamic relations (*27*).

The existence of mass- and heat-transport limitations was investigated a posteriori by diagnostic calculations (*28*). The results excluded interphase C- and T-gradients for our experimental conditions. Concerning resistances to intraporous diffusion, they were found to be negligible for C_1-linear growth (α) and ketonization (Γ), of small extent for β_N and β_B aldol condensations, and strong for β_E condensations (e.g., $C_2 \rightarrow C_3$ step). These results are consistent with the relative magnitudes of the rate parameters, as discussed in the following. In view of the other approximations introduced, we did not attempt to account specifically for such diffusional effects, which may cause β_N, β_B, and particularly β_E (and the corresponding activation energies) to be underestimated.

5. *Parameter Estimation*

The set of 42 mass balance equations (10) was integrated numerically by a self-adjusting stepsize ODE solver based on the implicit algorithm of Gear (*29*).

The optimal estimates of the nine kinetic parameters were determined by multiresponse nonlinear regression, using a specific optimization routine (*30*) based on several combined search procedures that ensured quick convergence. The task was minimizing the weighted squared deviations between calculated ($\hat{y}_{ij}$) and experimental (y_{ij}) exit molar concentrations of the 20 primary alcohols and ketones indicated in Table 3, ratioed to methanol concentration, and summed over all the kinetic runs. Each deviation was weighted with an estimate of the reciprocal variance of the corresponding response (s_i^2), obtained from few replicated runs.

$$S = \sum_{i=1}^{20} \sum_{j=1}^{N} (y_{ij} - \hat{y}_{ij})^2 / s_i^2. \qquad (12)$$

We recall that S (Eq. (12)) exhibits a χ^2 distribution with $20N - 9$ degrees of freedom if s_i^2 is replaced by σ_i^2, the expected value of s_i^2. However, due to the limited number of replicates available, the estimates of the error variance are to be regarded as very crude approximations of σ_i^2. The model adequacy was then evaluated essentially from the overall goodness of fit and from the physical consistency of the parameter estimates.

RESULTS AND DISCUSSION

1. *Data Fitting*

The histogram in Fig. 3 illustrates a typical model fit of the experimental ratios C_i/C_1.

Inspection of Fig. 3 indicates that the observed distributions of C_{2+} oxygenates can be quantitatively represented by the kinetic treatment of the present work. With respect to the complexity of the reacting system, and to the degree of approximation of the treatment, the goodness of fit appears to be satisfactory, in particular considering that the measured concentrations cover about three orders of magnitude. Errors are gen-

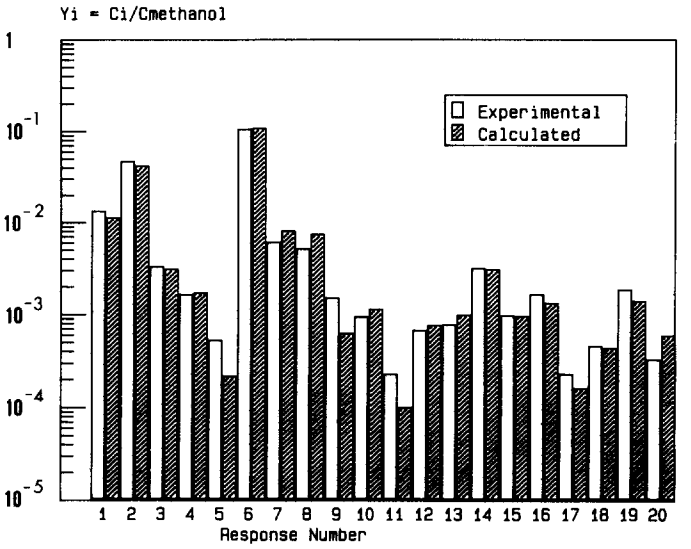

FIG. 3. Comparison between experimental and calculated C_{2+} oxygenates distributions over the Zn–Cr–O + 15% Cs_2O (w/w) catalyst. Reaction conditions: T = 385°C, P = 8.6 MPa, GHSV = 8000 h^{-1}, H_2/CO = 1/1, feed CO_2 = 0. Numbering of the responses as in Table 3. Parameter values as in Table 4.

erally below 20%, with the exceptions of 1-hexanol, 2-methyl-1-hexanol, and 3-methyl-1-pentanol, which are underestimated by roughly 40–50%. However, 1-hexanol and 3-methyl-1-pentanol are present in very small amounts, their concentrations being close to the experimental uncertainty.

Figure 4 shows how the kinetic treatment is able to handle the experimental effect of contact time on the concentrations of the oxygenated products at T = 385°C. Only the most representative species are shown in the figures. The values of the kinetic parameters are given in Table 4. Notably, linear species (ethanol, 1-propanol, 1-butanol, and 1-pentanol) approach a pseudo-steady-state behavior, but branched species (2-methyl-1-propanol and 2-methyl-1-butanol) do not.

Figure 5 indicates that also the effects of CO_2 addition to the syngas are correctly accounted for by the present treatment, which predicts a specific inhibiting influence of CO_2 on the yields of products (e.g., *i*-butanol), which do not undergo further sig-

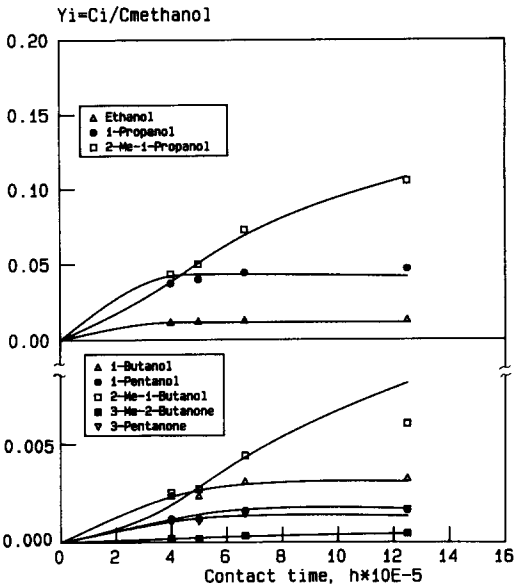

FIG. 4. Effect of contact time on the distribution of C_{2+} oxygenates over the Zn–Cr–O + 15% Cs_2O (w/w) catalyst. Reaction conditions: T = 385°C, P = 8.6 MPa, H_2/CO = 1/1, feed CO_2 = 0. Parameter values as in Table 4.

TABLE 4

Estimates at T = 385°C and Apparent Activation Energies of the Kinetic Parameters for the Reaction Network of HAS Chain Growth

Parameter	Estimated value at 385°C	Apparent activation energy (kJ/mol)
β_N ($h^{-1} \times 10^{-4}$)	2.23	15.5
β_B ($h^{-1} \times 10^{-4}$)	1.00	−3.8
β_E ($h^{-1} \times 10^{-4}$)	26.6	15.9
α ($h^{-1} \times 10^{-4}$)	0.384	64.9
Γ ($h^{-1} \times 10^{-4}$)	6.38	153.6
Ω	0.406	−55.2
Ω_{ORR}	0.923	22.6
Φ	0.116	−29.7
A_w	9.32	−300.1

Note. Reaction conditions as in Figs. 3, 7, and 8.

nificant aldol condensations. On the contrary, the concentrations of linear species (e.g., ethanol, 1-propanol, 1-butanol), which are not only formed but also consumed through aldol condensations, behaving essentially as intermediates in the chain growth, are marginally affected.

The observed strong reduction of the overall productivity of C_{2+} oxygenates is explained by the inhibiting action of water on the ORR mechanism, which is fully responsible for the $C_1 \rightarrow C_2$ growth step.

The present treatment cannot provide a global description of the product distribution as a function of the feed H_2/CO ratio or of the reaction pressure. In fact, the H_2- and CO-partial pressures affect the concentration of methanol, which is included in the definition of the rate parameters (Eqs. (11)). Furthermore, variations of the H_2 partial pressure modify the ratio of aldehydes to primary alcohols, as determined by hydrogenation equilibria. This also affects the estimates of the rate constants (e.g., α, β_N, β_E, β_B) appearing in rate expressions written in terms of alcohol concentrations rather than those of aldehydes, which are the true reactants. However, when the kinetic treatment was applied individually to each kinetic run corresponding to the different H_2/CO feed ratios and reaction pressures considered, an adequate fit of the single data set was obtained in all cases, with rate parameters exhibiting regular dependences on the experimental settings (see Table 5), which confirms the absence of incongruous situations in the process of data fitting.

It is also worth noting that the spectrum of oxygenates accounted for by the present model includes also aldehydes and secondary alcohols, related by hydrogenation equilibria to primary alcohols and ketones, as shown in Fig. 1. Since such equilibria are actually approached under HAS conditions, an accurate prediction of the concentration of a primary alcohol (or of a ketone) results also in a successful prediction of the corresponding aldehyde (or secondary alcohol), simply on the basis of the relevant equilibrium constant. The same considerations apply to methyl esters, which are also subject to the chemical equilibria discussed previously. Thus, it is concluded that the pres-

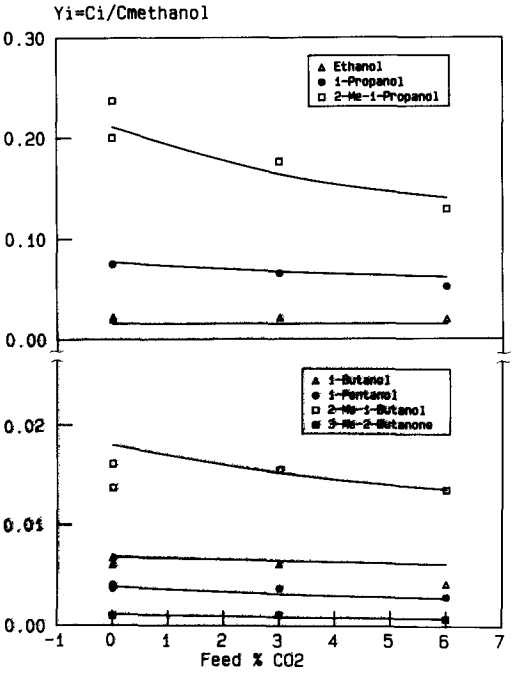

FIG. 5. Effect of CO_2-feed content on the distribution of C_{2+} oxygenates over the Zn–Cr–O + 15% Cs_2O (w/w) catalyst. Reaction conditions: T = 405°C, P = 8.6 MPa, GHSV = 8000 h^{-1}, H_2/CO = 1/1. Parameter values as in Table 5 for H_2/CO = 1/1.

TABLE 5

Effect of H_2/CO Feed Ratio on the Estimates of the Kinetic Parameters

Parameter	H_2/CO feed				
	1/2	1/1	2/1	4/1	1/1[a]
β_N ($h^{-1} \times 10^{-4}$)	2.76	2.14	2.07	1.78	3.25
β_B ($h^{-1} \times 10^{-4}$)	1.16	1.04	1.14	1.26	2.81
β_E ($h^{-1} \times 10^{-4}$)	46.2	30.6	22.4	14.9	32.7
α ($h^{-1} \times 10^{-4}$)	0.95	0.58	0.51	0.47	0.53
Γ ($h^{-1} \times 10^{-4}$)	18.2	18.6	16.9	18.8	17.1
Ω	0.13	0.28	0.31	0.44	0.41
Φ	0.08	0.09	0.10	0.12	0.21
A_w	4.14	0.97	≈0	≈0	0.03

Note. Reaction conditions: T = 405°C, P = 8.6 MPa, GHSV = 8000 h^{-1}, % CO_2 feed = 0. Ω_{ORR} was fixed at 1.04, as obtained from the analysis of data at H_2/CO = 1/1, to prevent instabilities in parameter estimation.

[a] P = 10.1 MPa, GHSV = 15,000 h^{-1}.

ent kinetic treatment is able to account for the concentrations of about 50 observed C_{2+} oxygenates: within the degree of approximation adopted, the resulting description of this complex product distribution appears to be quite close to reality. All the major detected oxygenates up to C_7 are described by the kinetic analysis.

An additional validation of the kinetic treatment is provided by inspection of the model predictions for about 50 additional compounds not included in the experimental responses of the regression. In fact, for several of them (e.g., acetone, 2,4-dimethyl-3-hexanone) the absence of the corresponding chromatographic peak parallels a very low model prediction for its outlet concentration, which is indeed below the measurement threshold of our analytical facilities (≈2 ppm).

Altogether, the kinetic analysis accounts for about 95% w/w of the total condensed products.

2. *Analysis of the Parameter Estimates*

Several remarks are in order upon examining the values of the rate parameters in the second column of Table 4.

1. The rate constant for C_1 linear addition (α) is nearly an order of magnitude smaller than β_N, the rate constant for normal aldol condensations. Since the rate of the $C_1 \rightarrow C_2$ step is proportional to ($\alpha\Omega_{ORR}$) and Ω_{ORR} is of order unity, the mechanism responsible for the first C–C bond formation is considerably slower than the ensuing condensations and represents the rate-determining step in the alcohol chain growth.

2. C_1 α-addition and C_i β-addition to a branched chain are remarkably slower than those to a linear one ($\Phi \ll 1$), because of electronic effects on the electrophilicity of the reactants or possibly because of steric hindrances. Steric and/or electronic effects adversely influence the rate of aldol condensations, too, as suggested by the comparison between β_B and β_N ($\beta_B < \beta_N$).

3. The rates of aldol condensations with normal and ORR modes are comparable, as shown by the value of Ω_{ORR} close to unity.

4. The very high value of β_E indicates a striking enhancement of the condensation rate in ORR mode associated with the $C_2 \rightarrow C_3$ step. Such an effect provides quantitative support to the data of Klier and co-workers (*5*), who observed a high C_3/C_2 ratio in the products of HAS over a Cs-promoted Cu/ZnO catalyst and attributed it to a relatively higher rate of the $C_2 \rightarrow C_3$ condensation step, specific of Cs-promotion. Similar results have been noted also in the case of high-temperature methanol synthesis catalysts (*26*).

5. In line with the chemistry of aldol condensations and with results of flow microreactor experiments with C_3 and C_4 oxygenates (*26*), the reactivity of aldehydes is greater than that of ketones, as shown by the value of Ω less than unity.

6. The positive sign of Γ confirms that ketones act as reactants in ketonization reactions, in agreement with the observed deviations from equilibrium (*16*). Its large value indicates that such reactions contribute significantly to the chain growth process.

7. The inhibiting effect of water on ORR condensations and ketonizations is remarkable, as shown by the value of A_W, and, in

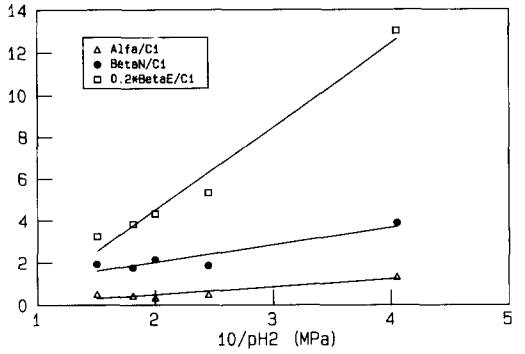

FIG. 6. Correlation of parameter estimates with partial pressure of H_2.

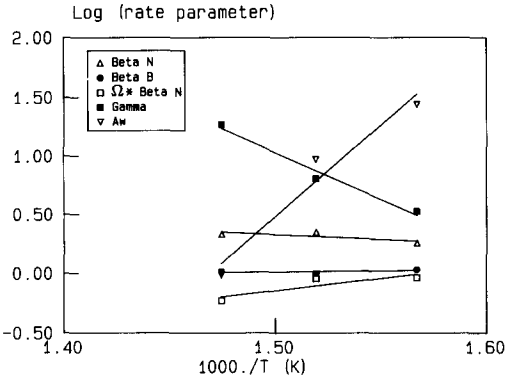

FIG. 7. Effect of reaction temperature on the estimates of the kinetic parameters. Reaction conditions: P = 8.6 MPa, GHSV = 8000 h^{-1}, H_2/CO = 1/1, CO_2 feed = 0.

conjunction with the WGS equilibrium, is responsible for the reduced productivity of C_{2+} oxygenates observed with CO_2-rich feed streams.

In Table 5, the rate constants β_N, β_E for aldol condensations and α for C_1 linear additions decrease with increasing H_2 feed content. This effect is related to a corresponding decrease of the concentrations of aldehydic reactants due to the modification of hydrogenation equilibria. As shown in Fig. 6, the estimates of such rate constants from Table 5, once divided by C_1 (i.e., the measured concentration of methanol), are inversely proportional to the H_2 partial pressure. When the rate constants of reactions involving ketones ($\Omega\beta_N$, $\Omega\beta_E$) were plotted as in Fig. 6, however, no dependence on p_{H_2} was apparent. In fact, in this case the concentrations of the actual reagents (i.e., ketones) were used in the rate expressions. The rate parameter for ketonization, Γ, and the rate constant ratio Φ are virtually unaffected by changes of syngas composition and pressure.

The influence of p_{H_2} on β_B and on A_W is less clear, as a greater uncertainty affects the estimates of such parameters. In the case of β_B, this is due to the limited number of responses affected by changes of its value. Concerning A_W, while reliable estimates could be secured from analysis of the series of runs with varying contact time and CO_2 feed content, which exhibited significant changes of the H_2O concentration in the products, strong correlations were noted with other parameters (Ω_{ORR}, Γ) in the case of regression on single runs.

Figures 7 and 8 illustrate the influence of the reaction temperature on the parameter estimates, which could all be satisfactorily correlated by Arrhenius plots for the three T-levels considered. The corresponding estimates of the apparent activation energies are also presented in Table 4.

It should be recalled that the rate parame-

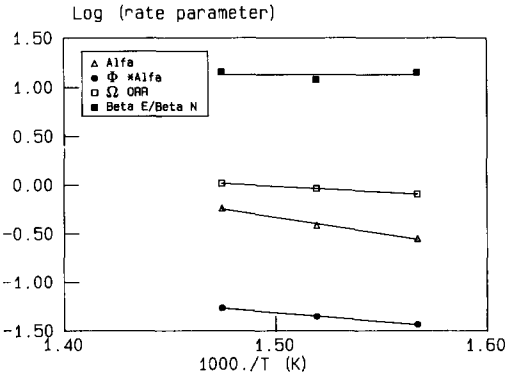

FIG. 8. Effect of reaction temperature on the estimates of kinetic parameters. Reaction conditions as for Fig. 7.

ters as defined in Eq. (11) incorporate also the T-dependences of the adsorption equilibrium constant and of the methanol concentration, as well as that of hydrogenation equilibria in those cases where the concentrations of primary alcohols instead of aldehydes have been used in the rate expressions. Assuming an inverse dependence of β_N on p_{H_2} as suggested by Fig. 6,

$$k'_{\beta,N} = \frac{\beta_N K_H p_{H_2}}{K_{ad} C_1} \qquad (13)$$

with $k'_{\beta,N}$ the intrinsic rate constant for aldol condensations and K_H the equilibrium constant for aldehyde–alcohol hydrogenation. Then,

$$E_{\beta,N} = E_{app,\beta,N} + \Delta H_H - \Delta H_{ads} - \Delta H_{C_1}, \qquad (14)$$

where $E_{\beta,N}$ and $E_{app,\beta,N}$ are the intrinsic and apparent activation energies of normal aldol condensations, respectively, ΔH_H is the enthalpy change of aldehyde hydrogenation reactions, ΔH_{ad} is the enthalpy of adsorption of the aldehydic species onto the catalyst, and ΔH_{C_1} is the enthalpy of formation of methanol from CO + H_2. Based on the following estimates,

$-63 \leq \Delta H_H \leq -88$ kJ/mol (*27*)

$-59 \leq \Delta H_{ads} \leq -88$ kJ/mol (*31, 32*)

$\Delta H_{C_1} = -102.1$ kJ/mol (*27*)

we obtain $71 \leq E_{\beta,N} \leq 142$ kJ/mol. The same considerations apply to the apparent activation energies of β_B and β_E, which are calculated in the range 54–142 kJ/mol, and of α 121–193 kJ/mol: thus, the estimates of the true activation energies of these rate parameters are positive in all cases, and exhibit plausible values for heterogeneously catalyzed reactions.

The three rate constants for aldol condensations (β_N, β_B, and $\beta_{N,K} = \Omega\beta_N$, where $\beta_{N,K}$ is the rate constant for aldol condensations involving ketones) share lower activation energies than those of the other paths, confirming that such reactions are relatively easy and fast under HAS conditions. However, the estimates of the activation energies for β-condensations are likely to be underestimated because of internal diffusional intrusions, particularly in the case of β_E. On the contrary, a significantly greater value has been found for the activation energy of the C_1 addition reactions, another indication that the $C_1 \rightarrow C_2$ step is the real bottleneck in the alcohol chain growth process.

Figure 8 shows that the ratios of rate constants $\Omega_{ORR} = \beta_{N,ORR}/\beta_N$ and β_E/β_N are not significantly affected by the reaction temperature, as expected.

The apparent activation energy of ketonization reactions is quite large. The existence of a sharp temperature threshold for the onset of ketone formation has been demonstrated by TPSR runs with C_4 oxygenates over a similar catalyst (*24, 25*).

According to Eq. (11), the value of the adsorption enthalpy of water onto the catalyst can be obtained subtracting ΔH_{C_1} ($= -102.1$ kJ/mol at 400°C) from the temperature coefficient of A_w in Table 4. The resulting figure (-198 kJ/mol) compares reasonably well with published data for the heat of dissociative adsorption of H_2O on metal oxide surfaces with strongly ionic nature. For example, values in excess of 151 kJ/mol have been measured calorimetrically on calcium oxide (*33*).

CONCLUSIONS

A kinetic treatment of HAS over Cs-promoted Zn–Cr oxide that overcomes limitations affecting previous attempts has been developed. It is now well known that the mechanism of alcohol chain growth over modified methanol synthesis catalysts is intrinsically different from the mechanism of the Fischer–Tropsch reaction, so that direct extension of the classical FT kinetic approach to the HAS seems inappropriate, and a specific approach is called for.

The reaction scheme incorporated in the present work takes advantage of the latest mechanistic findings on HAS and is fully consistent with the thermodynamic analysis of HAS product mixtures. Furthermore, by assuming adsorption equilibrium for the re-

agents, and releasing the pseudo-steady-state assumption for the concentrations of the intermediates, a description of the reacting system that is closer to the physicochemical reality of the synthesis over modified methanol catalysts is generated, involving reversible reaction steps as well as significant effects of contact time on the product distribution.

Considering also the relevant chemical equilibria, the model predicts the distribution of about 100 higher oxygenates as a function of contact time by means of nine adaptive parameters. For about 50 of these species a comparison is possible with data obtained from the analysis of product mixtures. With a few exceptions, the errors are comparable with the experimental uncertainty of the data.

The estimates of the kinetic parameters are consistent with the chemistry and the mechanistic features of the synthesis. In particular, the different reactivities in aldol condensations exhibited by molecules with different structures (e.g., ketones versus aldehydes), as reflected by the parameters required in the kinetic description, are found to be in line with available chemical data for homogeneous reactions and with independent mechanistic studies. The estimates of the temperature coefficients for the parameters are also acceptable. On this basis, the present treatment is able to accommodate the experimental influence of contact time, temperature and CO_2-feed content on the C_{2+} product distribution over a wide range of conditions. In its present form the kinetic model cannot account for the effects of changes in the feed H_2/CO ratio or in the total pressure. Nevertheless, the model is able to fit the product distributions of individual runs, with kinetic parameters varying as functions of H_2 partial pressures and of methanol concentration. The decrease of the parameter estimates with increasing p_{H_2} are consistent with the role of reactants attributed to aldehydic compounds in the chain growth mechanism.

In conclusion, the present work confirms the capability of the proposed reaction network, developed from independent measurements, and of the associated kinetic treatment to interpret on a quantitative basis the experimental complexity of HAS. The analysis also supports the existence of a chain growth route involving reverse ketonizations, which parallels the main route based on aldol condensations.

Notably, information can be extracted from the present treatment concerning the relevance of the various paths in the chain growth network. In particular, it is apparent from the results in Table 4 that the overall productivity to C_{2+} products can be increased only by reducing the activation barrier of the C_1 addition reactions involved in the first C–C bond formation and operating under conditions that prevent the inhibition of water on such reactions.

ACKNOWLEDGMENTS

Financial support from CNR (Roma), Progetto Finalizzato Chimica Fine/2, is gratefully acknowledged. The authors thank Snamprogetti SpA for technical assistance in the analysis of the product mixtures and Professor G. Buzzi-Ferraris for providing his multiresponse nonlinear regression program.

REFERENCES

1. Smith, K. J., and Anderson, R. B., *Can. J. Chem. Eng.* **61,** 40 (1983).
2. Klier, K., *in* "Catalysis on the Energy Scene" (S. Kaliaguine and A. Mahay, Eds.), p. 439. Elsevier, Amsterdam, 1984.
3. Vedage, G. A., Himelfarb, P. B., Simmons, G. W., and Klier, K., *ACS Symp. Ser.* **279,** 295 (1985).
4. Fornasari, F., Gusi, S., La Torretta, T. M. G., Trifirò, F., and Vaccari, A., *in* "Catalysis and Automotive Pollution Control" (A. Crucq and A. Frenuet, Eds.), p. 469. Elsevier, Amsterdam, 1987.
5. Nunan, J. G., Bogdan, C. E., Klier, K., Smith, K. J., Young, C. W., and Herman, R. G., *J. Catal.* **116,** 195 (1989).
6. Runge, F., and Zepf, K., *Brennstoff-Chem.* **35,** 167 (1954).
7. Riva, A., Trifirò, F., Vaccari, A., Busca, G., Mintchev, L., Sanfilippo, D., and Manzatti, W., *J. Chem. Soc. Faraday Trans. 1* **83,** 2213 (1987).
8. Tronconi, E., Ferlazzo, N., Forzatti, P., and Pasquon, I., *Ind. Eng. Chem. Res.* **26,** 2122 (1987).
9. Forzatti, P., Cristiani, C., Ferlazzo, N., Lietti, L., Pasquon, I., Tronconi, E., Villa, P. L., Antonelli, G. B., Sanfilippo, D., and Contarini, S., *in* "Actas 11th Iberoamerican Symposium on Catalysis" (F. Cossio, O. Bermudez, G. del Angel, and R. Go-

mez, Eds.), Vol. 2, p. 671. Guanojuato, Mexico, 1988; Forzatti, P., Cristiani, C., Ferlazzo, N., Lietti, L., Tronconi, E., Villa, P. L., and Pasquon, I., *J. Catal.* **111,** 120 (1988).
10. Tronconi, E., Lietti, L., Forzatti, P., and Pasquon, I., *Appl. Catal.* **47,** 317 (1989).
11. Forzatti, P., Tronconi, E., and Pasquon, I., *Catal. Rev.-Sci. Eng.*, **33,** 103 (1991).
12. Smith, K. J., and Anderson, R. B., *J. Catal.* **85,** 428 (1984).
13. Smith, K. J., Young, C. W., Herman, R. G., and Klier, K., *Ind. Eng. Chem. Res.* **29,** 61 (1991).
14. Tronconi, E., Forzatti, P., Groppi, G., Lietti, L., and Sanfilippo, D., *in* "Recent Advances in Chemical Engineering" (D. N. Saraf and D. Kunzru, Eds.), p. 217. Tata McGraw–Hill, New Delhi, 1989.
15. Tronconi, E., and Forzatti, P., *Chim. Ind. (Milan)* **70,** 66 (1988).
16. Tronconi, E., Forzatti, P., and Pasquon, I., *J. Catal.* **124,** 376 (1990).
17. Klier, K., Herman, R. G., Nunan, J. G., Smith, K. J., Bodgan, C. E., Young, C.-W., and Santiesteban, J. G., *in* "Methane Conversion" (D. M. Bibby, C. D. Chang, R. F. Howe, and S. Yurchak, Eds.), p. 109. Elsevier, Amsterdam, 1988.
18. Nunan, J. G., Bogdan, C. E., Klier, K., Smith, K. J., Young, C. W., and Herman, R. G., *J. Catal.* **113,** 410 (1988).
19. Elliott, D. J., and Pennella, F., *J. Catal.* **114,** 90 (1988).
20. Elliott, D. J., and Pennella, F., *J. Catal.* **119,** 359 (1989).
21. Lietti, L., Botta, D., Forzatti, P., Mantica, E., Tronconi, E., and Pasquon, I., *J. Catal.* **111,** 360 (1988).
22. Lietti, L., Tronconi, E., and Forzatti, P., *J. Mol. Catal.* **44,** 201 (1987).
23. Lietti, L., Tronconi, E., Forzatti, P., and Pasquon, I., *in* "Structure and Reactivity of Surfaces" (A. Zecchina, G. Costa, and C. Morterra, Eds.), p. 581. Elsevier, Amsterdam, 1989.
24. Lietti, L., Forzatti, P., Tronconi, E., and Pasquon, I., *J. Catal.* **126,** 401 (1990).
25. Lietti, L., Tronconi, E., Forzatti, P., and Busca, G., *J. Mol. Catal.* **55,** 43 (1989).
26. Lietti, L., Tronconi, E., Forzatti, P., *J. Catal.*, in press (1992).
27. Reid, R. C., Prausnitz, J. M., and Poling, B. E., "The Properties of Gases and Liquids," 4th ed. McGraw–Hill, New York, 1987.
28. Mears, D. E., *Ind. Eng. Chem. Process Des. Dev.* **10,** 541 (1971).
29. Hindmarsh, A. C., *ACM-Signum Newslett.* **15,** 10 (1980).
30. Buzzi-Ferraris, G., paper presented at the Working Party on Routine Computer Programs and the Use of Computers in Chemical Engineering, Florence, Italy, 1970.
31. Bowker, M., and Madix, R. J., *Appl. Surf. Sci.* **8,** 299 (1981).
32. Bowker, M., Houghton, H., and Waugh, K. C., *J. Catal.* **79,** 431 (1983).
33. Fubini, E., Bolis, V., Bailes, M., and Stone, F. S., *Solid State Ionics* **32/33,** 258 (1989).